Low temperature dielectric relaxation and charged defects in ferroelectric thin films

Alla Artemenko, Sandrine Payan, Anthony Rousseau, Delphin Levasseur, Emmanuel Arveux, Mario Maglione, Georges Guegan

Low temperature dielectric relaxation and charged defects in ferroelectric thin films

A. Artemenko, S. Payan, A. Rousseau, D. Levasseur, E. Arveux et al.

Citation: AIP Advances **3**, 042111 (2013); doi: 10.1063/1.4802242
View online: http://dx.doi.org/10.1063/1.4802242
View Table of Contents: http://aipadvances.aip.org/resource/1/AAIDBI/v3/i4
Published by the American Institute of Physics.

AIP ADVANCES **3**, 042111 (2013)

Low temperature dielectric relaxation and charged defects in ferroelectric thin films

A. Artemenko,[1,a] S. Payan,[1] A. Rousseau,[1] D. Levasseur,[1,2] E. Arveux,[1] G. Guegan,[2] and M. Maglione[1]
[1]*CNRS, ICMCB, UPR 9048, F-33600 Pessac, France*
[2]*STMicroelectronics, 16 Rue Pierre et Marie Curie 37071 Tours France*

(Received 21 February 2013; accepted 1 April 2013; published online 12 April 2013)

We report a dielectric relaxation in $BaTiO_3$-based ferroelectric thin films of different composition and with several growth modes: sputtering (with and without magnetron) and sol-gel. The relaxation was observed at cryogenic temperatures ($T < 100$ K) for frequencies from 100 Hz up to 10 MHz. This relaxation activation energy is always lower than 200 meV and is very similar to the relaxation that we reported in the parent bulk perovskites. Based on our Electron Paramagnetic Resonance (EPR) investigation, we ascribe this dielectric relaxation to the hopping of electrons among Ti^{3+}-V(O) charged defects. Being dependent on the growth process and on the amount of oxygen vacancies, this relaxation can be a useful probe of defects in actual integrated capacitors with no need for specific shaping. [http://dx.doi.org/10.1063/1.4802242]

I. INTRODUCTION

From the very beginning, the occurrence of charged defects has been recognized as a key issue for the optimization and long term use of ferroelectric films.[1] The low oxygen partial pressure during the vacuum films deposition, the cationic segregation in polycrystalline films and the oxygen diffusion during the films operation under electric stress are among the possible sources of such charged defects. Deep investigation of charged defects is underway including XPS, RBS/NRA measurements.[2–4] While the physics of defects in ferroelectric films has some specific features, it shares a lot of trends with related investigations in the parent bulk ferroelectric perovskites.[5] In single crystals and ceramics, from EPR spectroscopy or combining EPR and IR absorption,[6–10] clear evidence of polaronic states was observed, which is a highly probable outcome of charged defects and, in particular, oxygen-vacancies-related ones. We have previously shown that such polarons lead to a small but well defined dielectric relaxation in 100 different bulk perovskites of different compositions, morphologies and oxidation states.[11] Occurring always below 100 K in the sub-MHz frequency range, this relaxation is thermally activated with an activation energy lying in the 100 meV range.

In the present report, we show that low temperature ($T < 100$ K) relaxation observed in thin films of different composition obtained with several growth modes: sputtering (with and without magnetron) and sol-gel is also of polaronic type. This relaxation exhibits the same features as in the parent bulk compounds. Not only this result confirms the very microscopic origin of low temperature relaxation but it also establishes the use of dielectric spectroscopy as a simple tool for a qualitative classification of integrated ferroelectric capacitors with no need of specific shaping.

[a]Author to whom correspondence should be addressed: alla.artemenko@mail.ru

TABLE I. Thin films processing conditions, dielectric relaxation activation energy and the Ti^{3+}-V(O) defects density estimated from EPR.

Growth mode	Deposition conditions: (substrate or annealing temperature, atmosphere)	Samples number, (so-called in Fig. 4)	Films chemical composition	Dielectric relaxation activation energy, (meV)	Ti^{3+}-V(O) defects density, (cm^{-3})
Standard sputtering 2.5 $W.cm^{-2}$ 1.1Pa	Argon $T_{substrate}$ = RT	**SS**	$BaTiO_3$	50	10^{18}–10^{19} (from Ref. 15)
Magnetron sputtering 2.5 $W.cm^{-2}$ 5Pa	Ar/O_2 = 97.5/2.5 $T_{substrate}$ = 650 °C	**MS1**	$BaTiO_3$:Nb	85–150	10^{17} (this work)
	Ar/O_2 = 99/1 $T_{substrate}$ = RT post-annealing 650°C under O_2 flux	**MS2** **MS5**	$BaTiO_3$ $Ba_{0.6}Sr_{0.4}TiO_3$		
	Ar/O_2 = 99/1 $T_{substrate}$ = 650 °C	**MS3** **MS4**	$BaTiO_3$ $Ba_{0.6}Sr_{0.4}TiO_3$	~190	10^{15}–10^{16} (this work)
Sol-gel	annealed under O_2 at 800°C	**SG1** **SG2**	$BaTiO_3$ $Ba_{0.7}Sr_{0.3}TiO_3$		

II. EXPERIMENTAL

The ferroelectric films of different composition ("pure"/undoped $BaTiO_3$, Nb-doped $BaTiO_3$ and (Ba,Sr)TiO_3 [Ba/Sr = 70/30, 60/40 or 50/50], hereafter BT-based films) were grown on platinized silicon substrates of diverse origin. The first set of films was prepared by sputtering under different deposition conditions: with and without magnetron (hereafter MS or SS), deposition on a heated substrate or on room temperature substrate with subsequent post-annealing at 650°C under O_2 flux. As BT/BST target, a home-made 2-inches diameter ceramics was prepared by solid state reaction. $BaCo_3$ (Materion 99.9%), and TiO_2 (Materion 99.9%) powders were calcinated in O_2 at 1150°C for 5 hours and then the BT target was prepared by sintering during 4 hours at 1300°C under oxygen. The Nb concentration in the target was 0.05%wt. In the case of BST, powders of the same origin were first synthesized from stoichiometric mixtures of $BaCO_3$, $SrCO_3$ and TiO_2, calcinated in O_2 at 1200°C for 5 hours and then the target was prepared by sintering during 4 hours at 1350°C under oxygen. All films were deposited onto 10*20 mm^2 Pt/Si wafers, placed at 80 mm above the target at a fixed RF power density (2.5 or 1 $W.cm^{-2}$) and a constant pressure of 5 Pa. The plasma base gas was argon enriched with oxygen to 99:1 or 97.5/2.5 Ar/O_2 ratio. As-prepared films were polycrystalline, totally disoriented with 50 nm average grain sizes. The second set of films was deposited by sol-gel (SG) spin coating on platinized silicon wafers of 6 inch in diameter. The sol used for the deposition is industrial (from Mitsubishi Material Corp. Japan) and high purity. After spinning the films were pyrolyzed on a hot plate and then crystallized at 800°C in O_2. Table I summarizes films deposition conditions.

In addition to the compositional changes, the investigated films are very diverse: while sputtered films are textured with several preferred orientation, sol-gel films have random orientation. The columns diameter in sputtered films and the grain size in sol-gel films lie in the sub-100 nm range. The thickness of the obtained films is in the range of 230–340 nm.

Platinum dots were deposited at the surface for dielectric measurements in the Metal-Insulator-Metal (MIM) geometry. Using a quantum design dewar the sample temperature could be monitored from 4 K to 340 K with an accuracy better than 0.1 K. The operating frequency has been swept from 100 Hz to 10 MHz.

Electron Paramagnetic Resonance (EPR) measurements were performed at standard Bruker spectrometer operating at frequency 9.4 GHz utilizing a TE_{102} rectangular microwave cavity with

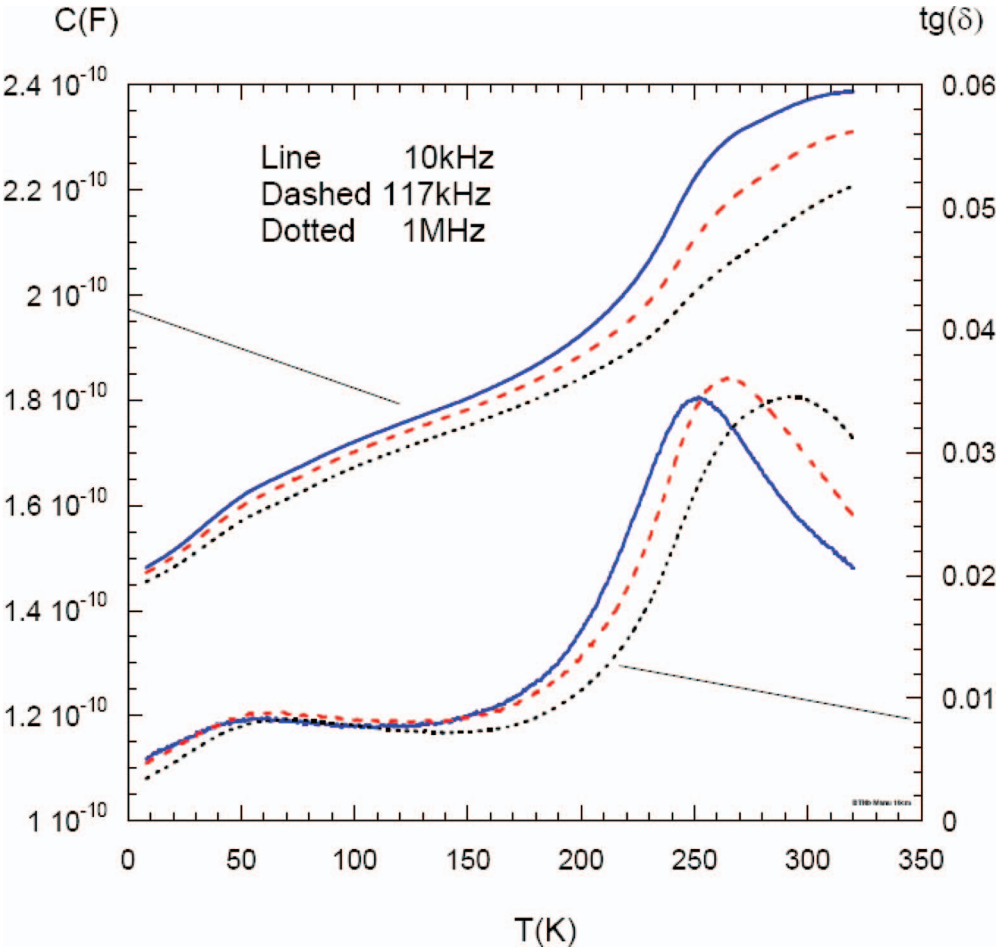

FIG. 1. Typical temperature variation of capacitance (left scale) and dielectric losses (right scale) for selected spot frequencies for the magnetron sputtered Nb-doped $BaTiO_3$ film showing an interface relaxation at high temperature ($T > 230$ K) and another relaxation for lower temperature ($T < 100$ K).

100 kHz magnetic field modulation. The samples have been pasted on the quartz tube and placed in an Oxford Instruments ESR 900 continuous-flow helium cryostat inside the microwave cavity that allow performing rotation experiments as well as the temperature dependence study. The temperature could be varied and controlled over the temperature range 4 to 300 K.

III. RESULTS AND DISCUSSION

Since the processing and post-processing annealing took place at different temperatures and atmospheres, we can expect a different density of oxygen vacancies in all films. Thanks to complementary EPR investigations, we have identified charged defects, estimate their concentration and further show how these defects directly impact ferroelectric thin films dielectric properties, in particular, the low temperature relaxation. As an example, a typical variation of capacitance and dielectric losses is shown in Figure 1 for selected spot frequencies and for the whole temperature range for a sputtered Nb-doped $BaTiO_3$ film. In this figure, two anomalies are clearly evidenced at about 250 K and 50 K. We will first focus on the high temperature feature which was already reported in several papers[12,13] for $BaTiO_3$ films with different electrodes. The maximum in losses can be ascribed to a dielectric relaxation whose activation energy is computed from an Arrhenius law linking the operating frequency f to the related temperature T where the loss maximum occurs $f = f_0 e^{-E/kT}$. The activation energy for this high temperature relaxation is about 100 meV in all

cases. We ascribe this temperature to space charge localization at electrodes/film interfaces[11] and we exclude any intrinsic origin for it.[14] Because of its large variability, this interface related relaxation will not be discussed further.

We rather focus now on the low temperature dielectric relaxation recorded in all of the 15 investigated films. Typical loss maximums are shown for sputtered and sol-gel BST films at the frequency range of 10 kHz–10 MHz (correspondingly Figure 2(a) and 2(b)). As for the high temperature relaxation, pointing the temperature at which the maximum occurs for a given frequency leads to a set of (f, T) couples which can be plotted in an Arrhenius law f vs 1/T using a semi-logarithmic scale.

Arrhenius plot together with their fit with equation $f = f_0 e^{-E/kT}$ are displayed in Figure 3 where f_0 is the high temperature extrapolation of the relaxation frequency f, E its activation energy and k the Boltzmann constant. We first underline that the Arrhenius law holds for all of the investigated films and that the activation energy is always below 200 meV. The extrapolated high temperature frequency f_0 is very much fluctuating because of the limited and low temperature range where the relaxation takes place. We will thus now discuss the computed activation energies and their possible link with the films processing, structure and charged defects content.

In Figure 3, one can see that these activation energies are of the same order (<200 meV) as the one already reported in a large number of bulk perovskites whatever their morphology (ceramics or single crystals), composition, doping and ferroelectric properties.[11] Such persistence called for a common origin which was ascribed to dipolar relaxations between polaronic type defects. These polarons can originate from charged point defects which are always present in oxides; even the purest single crystals contain residual impurities (Fe, Mn, Cr, Ni etc.) or oxygen vacancies. In particular, polaronic type relaxation between oxygen-vacancy-related defects (Ti^{3+} - V(O)) was evidenced in textured BT thin films.[15] Even though such polaron model is still under discussion,[16–18] we can transfer it to our thin films since the atomic density of oxygen vacancies remains high in both vacuum deposited and sol-gel processed films. Within this general model, we try now to sort the activation energies that we found versus the processing conditions keeping in mind that the key for the polaron relaxation to occur is the stabilization of charged point defects:

- the lowest activation energies are found for $BaTiO_3$ films which were room temperature sputtered using a standard radio frequency sputter deposition without or with bias that was applied to the substrate during the growth. EPR experiments previously shown that such columnar films contain a lot of oxygen vacancy-related defects like Ti^{3+}-V(O);[15] when a bias was applied to the substrate during the growth, the density of such defects was shown to be the highest and this is the case of non-magnetron sputtered films which show the lowest activation energy of 10 meV. For these films, we ascribe the extremely low activation energy to the easy hopping of polarons among very closely spaced charged defects.
- intermediate activation energies occur in magnetron sputtered films which were high temperature processed either during the growth or post-annealed after room temperature deposition. In these BT-based films the activation energy is increasing with the disorientation degree of the films from about 80 meV up to 150 meV. Since magnetron sputtered films are closer to stoichiometry than the non-magnetron sputtered film mentioned above, lower density of charged defects can be assumed in the former case.
- for all BT-based sol-gel films the activation energy is always in the higher range which is in between 160 and 195 meV; this may be related to the lowest density of charged defects and hence low hopping probability of polarons in such optimized films.

Having established a classification of the relaxation activation energies, we look in the following for their microscopic origin. As already shown in bulk crystals, ceramics and nanopowders, Electron Paramagnetic Resonance is the right tool for achieving this goal.

EPR studies were performed on similar films deposited on silicon substrates (same compositions, same growth mode). Together with our previous report on non-magnetron Standard sputtered BT films[15] we thus have a full set of EPR data on the same films that were probed for their dielectric relaxation. The statistical distribution of charged defects in each film was checked by probing several randomly selected pieces all of 2×4 mm^2 surface and with even homogeneous thickness. Figure 4

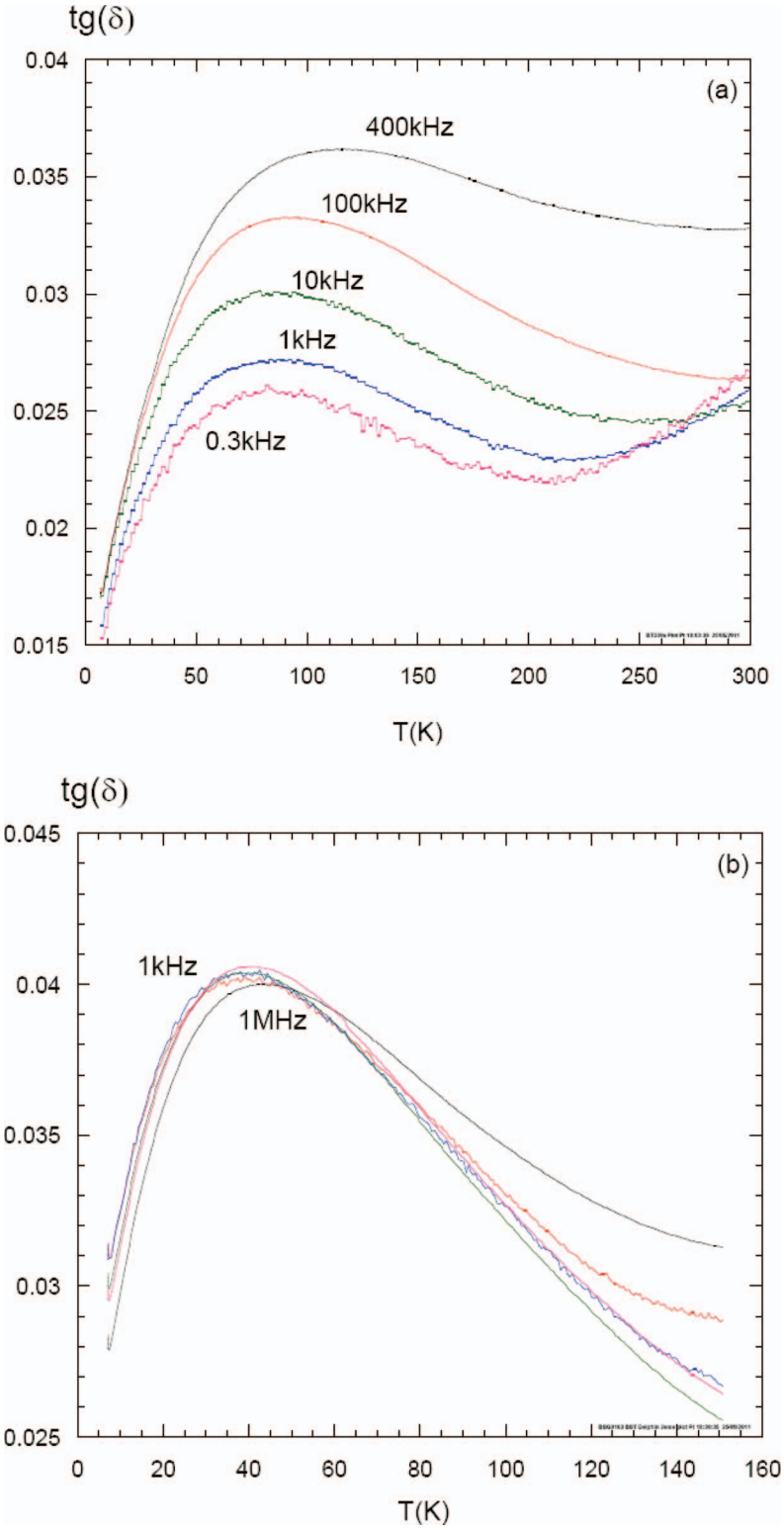

FIG. 2. Low temperature relaxation of BT-based film deposited using magnetron sputtering (a) and sol-gel (b). Spread of the loss peak over temperature is larger in the former case showing lower activation energy.

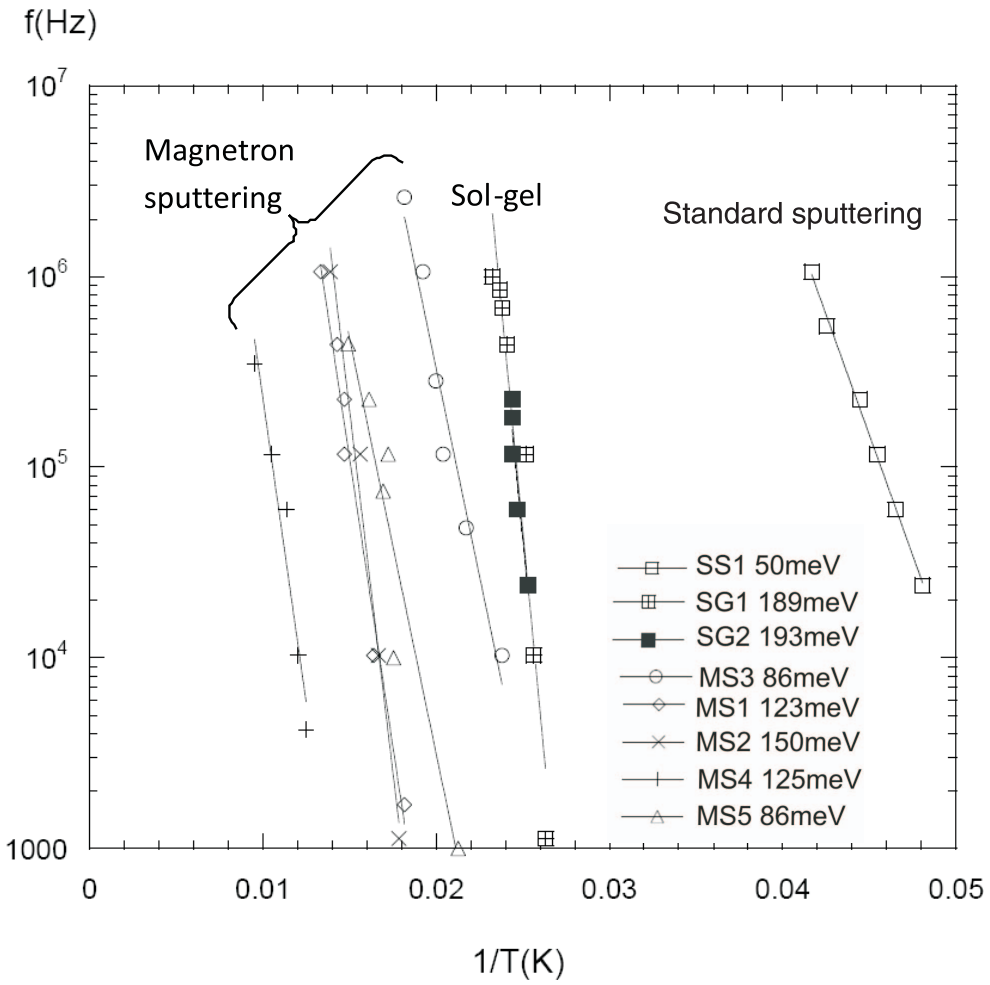

FIG. 3. Relaxation map for several of the investigated BT-based films: SS (standard sputtered films without magnetron and without substrate heating); MS1, MS2, MS3, MS4, MS5 (magnetron sputtered films with substrate heating or post-annealing); SG1, SG2 (sol gel deposited films). Sample references together with their activation energies calculated from Arrhenius fitting are reported in Table I. Obtained values of the activation energies are the highest for sol gel films and the smallest for standard sputtering ones, reflecting lowest defects density in SG films.

shows the plots for EPR spectra recorded at 10 K for the standard sputtered (SS), magnetron sputtered (MS) and sol-gel (SG) films as well as for powder made from the dehydrated-sol. For both films a resonance arising from (unavoidable) Fe^{3+} impurity is visible. Spectra collected for sol-gel films also contain intensive resonances that are ascribed to Mn^{2+} impurity; its origin in the sol is evidenced with the data from the sol powder that exhibit a similar signal. Both Fe^{3+} and Mn^{2+} impurities are substituted for Ti^{4+} and are partly compensating charge deficiency related to the oxygen vacancies. These impurities' concentration estimated from EPR intensity, does not exceed few tens ppm and they are hardly expected to strongly influence the films properties. In addition to these resonances, some other are observed in all films in the magnetic field region 340-360 mT.

In our previous report, we already ascribed these resonances to oxygen-vacancy-related defects; the link between these charged defects, their valence state and materials properties was also established, in particular, their strong impact on dielectric losses.[19–22] Within this context, the approach applied for ceramics and nanopowders is reasonably extending to thin films. Just like in the case of BT-based films in this study, the BT thin films in Ref. 15 were deposited on Si or amorphous SiO_2 substrates. Due to similar deposition conditions here and in, Ref. 15, the same type of charged defects is expected and together with both the identical position of the resonances and the equal ratios

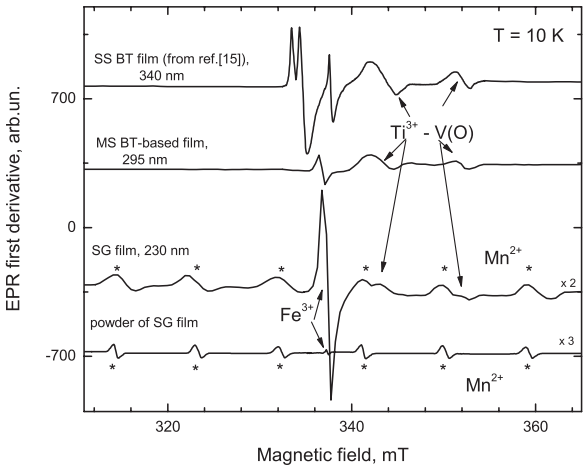

FIG. 4. EPR spectra recorded at T = 10 K for standard sputtered BT film from Ref. 15 (top plot) and BT-based films made using magnetron sputtering and sol gel; the spectrum recorded on sol-gel powder (bottom plot). For better resolution, the signal intensity for the sol gel film and for the powder made from the sol is multiplied by factor 2 and 3 respectively.

between them, it allows here also to reasonably ascribe the present resonances to oxygen vacancy related defects. The Ti^{3+}-V(O) charged defects activation energy calculated from the T-dependence of the EPR line-width is close to the one obtained from dielectric measurements. The specific conditions of films preparation (temperature, atmosphere, pressure, post deposition treatments etc.) are key points for the control of the charged defects density. For the present BT-based films, either magnetron sputtered or sol-gel, the difference stands in the temperature and atmosphere conditions (SG: 800°C / O_2; MS: 650°C / 99% Ar + 1% O_2 / P = 5 Pa; powder made from the dehydrated-sol was annealed at 1000°C / O_2). Thus, lower oxygen vacancies concentration is expected in sol-gel films. In addition, sol-gel films contain both Fe^{3+} and Mn^{2+} impurities which substitute for Ti^{4+} ions and can further partly compensate for the oxygen deficiency. In the case of standard sputtered BT films the concentration of Ti^{3+} - V(O) defects was estimated to be 10^{18}–10^{19} cm^{-3}.[15] Using this value as a reference and taking into account the difference in the films thickness and the evolution of the intensities in Fig. 4, the concentration of these defects is estimated to be 10^{17} cm^{-3} and 10^{15}–10^{16} cm^{-3} for the magnetron sputtered and sol-gel films, respectively. This trend is quite consistent since the amount of oxygen vacancy related defects is to decrease when using sol-gel for which all annealing take place under oxygen while sputtering is a vacuum process. We already demonstrated that in $BaTiO_3$, Ti^{3+} - V(O) charged defects create an energy level close to the bottom of the conduction band which enhances the grain conductivity through electronic hopping[9] and the same process logically applies to BT-based films. Instead of stemming from standard localized dipoles, we thus suggest that the dielectric relaxation results from the electron hopping among the Ti^{3+} - V(O) centers. If the relaxation activation energy is linked to the hopping probability, it should increase when decreasing the density of defects, which increases the average distance between them. This is clearly confirmed in Table I where one can compare dielectric relaxation activation energies and density of Ti^{3+}-V(O) for all investigated films.

IV. SUMMARY

To summarize, we have shown that a small amplitude dielectric relaxation is always observed at cryogenic temperature in ferroelectric perovskite thin films. This observation is very similar to what was reported in a large number of bulk materials of the same family. The relaxation occurs in all films whatever their morphology, texture, chemical content and processing way. We mapped out the relaxation activation energies of the films deposited by different methods with the amount of charged defects. In the case of magnetron sputtered films deposition onto high temperature substrate or on room temperature substrate with subsequence crystallization, sputtering at various Ar/O_2 gas mixing

ratios (1 or 2.5% of O_2), is just varying the activation energy from 85 to 150 meV. This value it still between one calculated in the case of standard sputtered and sol-gel films, revealing that defects density is the key point in low temperature dielectric relaxation. Our EPR investigations shown that Ti^{3+}-V(O) defects are always present in all BT-based films and that their density increases when moving from oxygen-annealed sol-gel films towards vacuum-grown films. We thus could link the increase of the dielectric activation energy to the decrease of the defects density. We ascribe such a link to the lower electrons hopping probability among Ti^{3+}-V(O) centers when the average distance between such defects increases. Beyond this preliminary model, low temperature dielectric and EPR spectroscopies might appear as simple tools –albeit non quantitative– for classifying integrated ferroelectric capacitors with no need for a specific shaping or preparation prior to the investigation. This could be helpful in the process of ferroelectric films properties optimization, for instance, to control their dielectric losses and leakage current.

ACKNOWLEDGMENTS

This work was supported by the European Multifunctional Materials Institute (EMMI), the Conseil Régional d'Aquitaine and the French National Agency for Research under the project ANR ABSYS (Grant no ANR-08-BLAN-0277). A.A. acknowledges the financial support by the European project ''EPREXINA'' under Marie Curie actions (Grant no. PIIF-GA-2009-255662). We also thank Rodolphe Decourt (ICMCB) who has built a measurement setup for cryogenic temperature dielectric experiments on thin films. Solutions used for the sol-gel films processing were provided by Mitsubishi Corp. Japan.

[1] J. F. Scott, *Ferroelectric Memories*, Advanced Microelectronics Vol. 3 (Springer, Heidelberg, 2000).
[2] O. Auciello, A. Dhote, R. Ramesh, B. T. Liu, S. Aggarwal, A. H. Mueller, N. A. Suvarova, and E. A. Irene, Integrated Ferroelectrics **46**, 295–306 (2002).
[3] J. D. Baniecki, M. Ishii, T. Shioga, K. Kurihara,and S. Miyahara, Appl. Phys. Lett. **89**, 162908 (2006).
[4] R. Schafranek, S. Payan, M. Maglione, and A. Klein, Phys. Rev. B **77**, 195310 (2008).
[5] K. Szot, F. U. Hillebrecht, D. D. Sarma, M. Campagna, and H. Arend, Appl. Phys. Lett. **48**, 490 (1986).
[6] S. Lenjer, O. F. Schirmer, H. Hesse, and Th. W. Kool, Phys. Rev. B **66**, 165106 (2002).
[7] V. A. Trepakov, A. I. Gubaev, S. E. Kapphan, P. Galinetto, F. Rosella, L. A. Boatner, P. P. Syrnikov, and L. Jastrabik, Ferroelectrics **334**, 113 (2006).
[8] V. V. Laguta, A. M. Slipenyuk, I. P. Bykov, M. D. Glinchuk, M. Maglione, A. G. Bilous, J. Rosa, and L. Jastrabik, J. Appl. Phys. **97**, 073707 (2005).
[9] A. Artemenko, C. Elissalde, U-C. Chung, C. Estournès, S. Mornet, I. Bykov, and M. Maglione, Appl. Phys. Lett. **97**, 132901 (2010).
[10] C. Elissalde, U-C. Chung, A. Artemenko, C. Estournes, R. Costes, M. Pate, J.-P. Ganne, S. Waechter, and M. Maglione, J. Am. Ceram. Soc. **95**, 1–7 (2012).
[11] O. Bidault, M. Maglione, M. Actis, M. Kchikech, and B. Salce, Phys. Rev. B **52**, 4191 (1995).
[12] O. Trithaveesak, J. Schubert, and Ch. Buchal, J. Appl. Phys. **98**, 114101 (2005).
[13] Liang Qiao and Xiao fang Bi, J. Phys. D: Appl. Phys. **42**, 175508 (2009).
[14] E. Arveux, thesis Bordeaux, Darmstadt (2009), http://tel.archives-ouvertes.fr/tel-00461201/fr/.
[15] V. V. Laguta, A. M. Slipenyuk, I. P. Bykov, M. D. Glinchuk, M. Maglione, D. Michau, J. Rosa, and L. Jastrabik, Appl. Phys. Lett. **87**, 022903 (2005).
[16] J. F. Scott, A. Q. Jiang, S. A. T. Redfern, Ming Zhang, and M. Dawber, J. of Appl. Phys. **94**, 3333 (2003).
[17] J. L. M. van Mechelen, D. van der Marel, C. Grimaldi, A. B. Kuzmenko, N. P. Armitage, N. Reyren, H. Hagemann, and I. I. Mazin, Phys. Rev. Lett. **100**, 226403 (2008).
[18] T. Kolodiazhnyi and S. C. Wimbush, Phys. Rev. Lett. **96**, 246404 (2006).
[19] M. D. Glinchuk, I. V. Kondakova, V. V. Laguta, A. M. Slipenyuk, and I. P. Bykov, Acta Phys. Pol. A **108**, 47–60 (2005).
[20] M. D. Glinchuk, A. N. Morozovska, A. M. Slipenyuk, and I. P. Bykov, Appl. Mag. Reson. **24**, 333–42 (2003).
[21] A. M. Slipenyuk, I. V. Kondakova, M. D. Glinchuk, and V. V. Laguta, Phys. Status Solidi C **4**, 1297–300 (2007).
[22] R. Waser and M. Klee, Integr. Ferroelectrics. **2**, 23 (1992).